Journal of the European Ceramic Society 19 (1999) 1987–1996

PII: S0955-2219(99)00012-6
0955-2219/99/$ - see front matter

Influence of CO_2 in Dry and Wet Atmospheres on the Response of Mg-doped $SrTiO_3$ Ceramic Oxygen Sensors

Hong Zheng* and O.Toft Sørensen

Materials Research Department, Risø National Laboratory, PO Box 49, DK-4000 Roskilde, Denmark

(Received 12 October 1998; accepted 30 December 1998)

Abstract

Mg-doped $SrTiO_3$ thick film sensors fabricated by screen-printing proved to be very promising for the use as oxygen sensors. The resistance of such sensors exhibits a P_{O_2} dependence according to $R \propto P_{O_2}^{-1/4}$. The influence of CO_2 in dry and wet atmospheres was evaluated in this work. The results obtained show that the presence of CO_2 has no influence on the oxygen-sensing properties of the sensor in dry conditions and the Mg-doped $SrTiO_3$ sensor can work even better than the ZrO_2 oxygen sensor in the dry CO_2-containing atmospheres. In an atmosphere containing both CO_2 and H_2O, the Mg-doped $SrTiO_3$ sensor can only operate properly as oxygen sensor at CO_2 concentrations below 70%. The effects from CO_2 and H_2O become stronger at CO_2 contents higher than 80%. An interesting CO_2-sensing characteristic instead of oxygen-sensing of the Mg-doped $SrTiO_3$ sensor is observed in a wet non-oxygen atmosphere. A model based on the defect chemistry, grain structures and conduction mechanisms of this material is developed in order to explain the experimental results. It is proposed that CO_2 may be absorbed at the surface of this oxide and an uncharged complex is formed in the dry conditions. In the presence of H_2O, a partial proton conduction is introduced to the total conductivity due to the surface reactions between CO_2 and H_2O. This material may become a predominant proton conductor in a non-oxygen atmosphere containing both CO_2 and H_2O.

Keywords: oxygen sensor, proton conduction, $SrTiO_3$, sensors.

*To whom correspondence should be addressed at present address: Department of Engineering Materials, University of Sheffield, Sheffield S1 3JD, UK. Fax: +44-(0)114-222-5943; e-mail: mtp98hz@sheffield.ac.uk

1 Introduction

Interest is currently growing in simple-to-manufacture, low-cost oxygen sensors for the applications as exhaust gas sensors in the automotive industry and for monitoring furnace installations.[1] In the temperature range above 600°C, some semiconductor metal oxides such as $SrTiO_3$, CeO_2 are suitable for detecting changes in oxygen partial pressure of the surrounding atmosphere.[2] Compared to the commercial solid-electrolyte ZrO_2 oxygen sensors, the semiconducting-type oxygen sensors surely have profits with respect to simple fabrication (thick-film technology), easy operation (no need for reference gas), small size, quick response and they also have the potential to be produced at low costs. As reported in our previous work,[3] sensors based on semiconductor oxide Mg-doped $SrTiO_3$ show good oxygen-sensing properties in the PO_2 region from 10^{-5} to 10^{-1} bar in an atmosphere containing only N_2 and O_2. The oxygen-sensing mechanism of this oxide at high temperatures is considered as a bulk effect based on a thermodynamic equilibrium between the oxygen in the surrounding atmosphere and the oxygen vacancies presented in this material. Normally, Mg-doped $SrTiO_3$ exhibits *p*-type hole conducting characteristic in this considered PO_2 region and electron holes are formed according to the following reaction:

$$\frac{1}{2}O_2 + V_O^{\bullet\bullet} \longleftrightarrow O_O^{\times} + 2h^{\bullet} \qquad (1)$$

where $V_O^{\bullet\bullet}$ represents an oxygen vacancy and $h^{\bullet}$ represents an electron hole.

According to this reaction, the relationship between the resistance of the sensor and the oxygen partial pressure of the surrounding atmosphere can therefore be described by the expression:[4]

$$R = A_1 \exp(E_p/kT) P_{O_2}^{-1/4} \quad (2)$$

where A_1 is a constant, E_P is the thermal activation energy for hole conduction.

A plot of $\log R$ versus $\log P_{O_2}$ should thus result in a straight line with a slope$(-1/m)$ of $-1/4$ at constant temperatures as shown in eqn (3):

$$\log R \propto -1/4 \log P_{O_2} \quad (3)$$

However, under practical field conditions, the gas atmosphere often contains other components in addition to oxygen and nitrogen, among which CO_2 and H_2O are regarded as the most possible interfering gases. Considering the possible chemical reactions, these gaseous components may either change the oxygen partial pressure of the atmosphere or generate or annihilate the bulk and surface defects of this oxide.[5] The presence of these gases thus has a direct effect on the electrical behaviors of the sensors. In this work, the Mg-doped $SrTiO_3$ oxygen sensors were fabricated by screen-printing and the influence of CO_2 on the response of such sensors was examined both in dry and wet atmospheres. Some theoretical considerations based on defect chemistry, grain structures and conduction mechanisms of this material were also carried out in order to interpret the experimental results.

2 Experimental

2.1 Preparation and characterisation of the Mg-doped $SrTiO_3$ powder

The details of the preparation of Mg-doped strontium titanate powder was described in our previous work.[6] The Mg-doped $SrTiO_3$ powder obtained was examined by X-ray diffraction (XRD) and it was confirmed that this powder was highly crystallised in a dominating structure of perovskite similar to undoped $SrTiO_3$ as shown in Fig. 1. The XRD pattern turns out that magnesium has been dissolved into strontium titanate structure, forming a solid solution. Some small traces of another phase can be also observed in the X-ray diffraction pattern. However the presence of this phase is not considered important in the interpretation of the results obtained in this work. This powder was used for sensor fabrication.

2.2 Sensor fabrication by screen-printing

Recently, the well-known advantages of screen-printing technology in microelectronics, such as versatility in sensor design, miniaturisation, mass production at low cost are also applied to the field of chemical sensing.[7] In this process, a paste of sensor material suitable for printing is usually required and the paste used in this work was prepared by mixing 55% wt% of the Mg-doped $SrTiO_3$ powder with 45% wt% of organic binder. A commercial platinum paste was used for the fabrication of electrode films.

A layer of Mg-doped $SrTiO_3$ was first screen-printed on a $50\times50\times0{\cdot}25\,mm^3$ alumina substrate and fired at a maximum temperature of 1200°C for 2 h. On top of this film, a platinum electrode film was subsequently screen-printed and fired at 1000°C for 1 h. The width between two platinum electrodes was 400 μm. Then sensors of the required size ($5\times8\times0{\cdot}25\,mm^3$) were obtained by laser cutting the substrate. The structure of a screen-printed Mg-doped $SrTiO_3$ sensor was shown in Fig. 2. Finally, platinum wires, serving as the leads, were fixed with platinum paste on each individual sensor and then heat-treated once more to 900°C for 1 h. After printing and sintering, the platinum electrode film had a typical thickness of about 10 μm and the Mg-doped $SrTiO_3$ film had a typical thickness of about 80 μm.

2.3 Measurement set-up

The set-up for sensor testing is schematically illustrated in Fig. 3.

Two samples were placed in two tube furnaces respectively, where the sample temperature could be changed by adjusting the voltage of the furnace heater and the actual sample temperature was measured with a thermocouple, which was placed alongside the sample. A ZrO_2 sensor was used to check the oxygen partial pressure of the carrier gas.

With aim to evaluate the influence of CO_2 on the oxygen-sensing properties of the sensors, test gas of different oxygen partial pressures (10^{-4} bar $< P_{O_2} < 0{\cdot}21$ bar) was obtained by diluting air with CO_2 gas. Gases with various CO_2 concentrations were prepared by diluting CO_2 with air or N_2 gas and the CO_2 concentration of the test gas was determined by the dilution calculation ranging from 6 to 100%. Wet gases used in these tests were the water-saturated gases by passing through a H_2O bubbler at 25°C. The gas flow past the sample was controlled by a flowmeter, which was set at a constant rate of 100 cc min^{-1}.

The signals of the resistance and the temperature of these two Mg-doped $SrTiO_3$ sensors, the EMF signal of the ZrO_2 sensor were collected simultaneously by the Signalogger-PC. Signalogger-PC is an eight channel datalogger system comprising a small hardware unit (the interface) and the software for the host computer. It can accept a variety of inputs at sampling rates from one per second to one per hour. The data can be directly displayed on

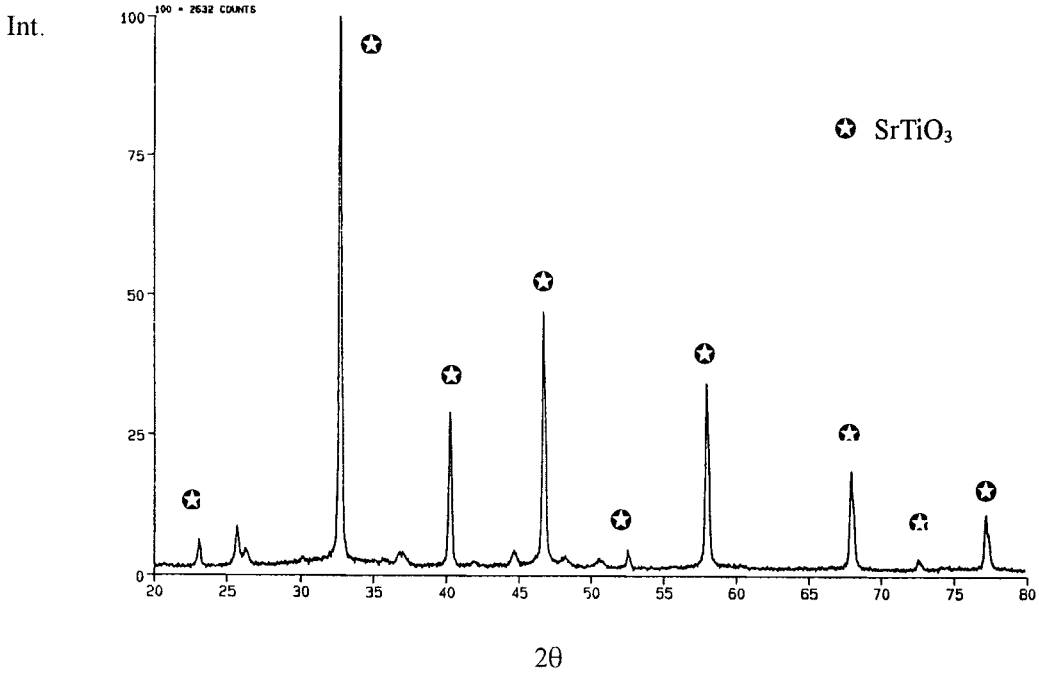

Fig. 1. X-ray diffraction pattern of the Mg-doped $SrTiO_3$ powder.

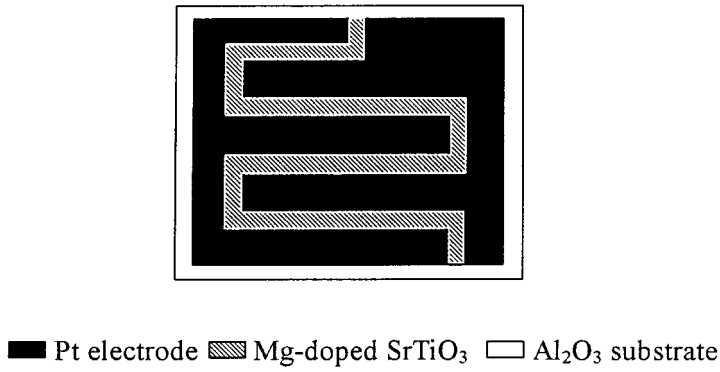

Fig. 2. Structure of a screen-printed Mg-doped $SrTiO_3$ sensor element.

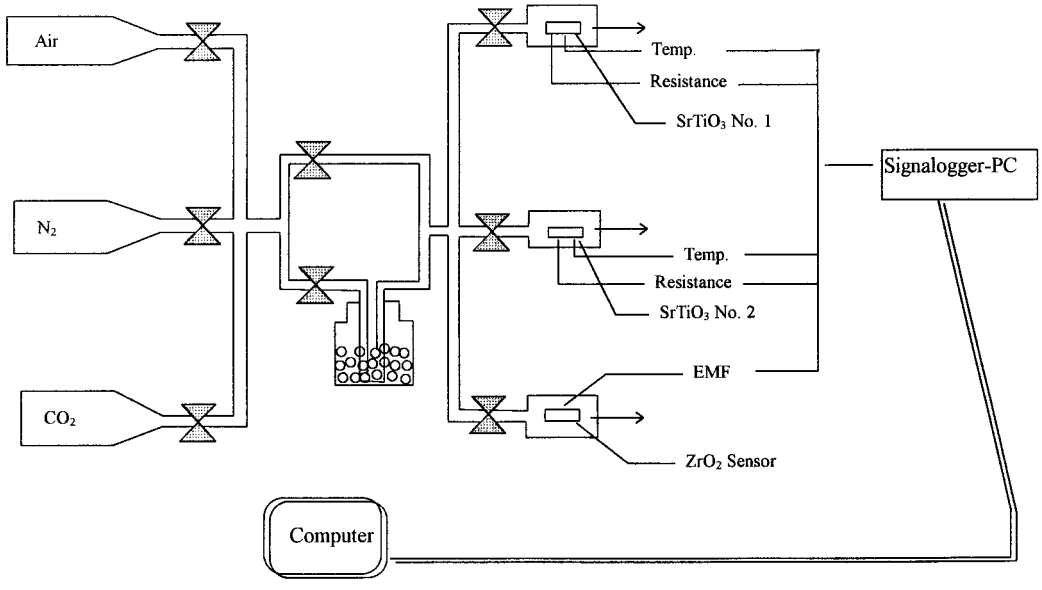

Fig. 3. Schematic illustration of the measurement set-up.

the host computer at any measuring time and the results can be saved to disk or printed out on a standard printer.

3 Model of the Grain Structures of Mg-Doped $SrTiO_3$

For further interpreting the surface chemisorption process of the sensors, it is helpful to develop a model for the grain structures of Mg-doped $SrTiO_3$.

In recent literature on titanates, it has been widely accepted that the transition between two grains can be viewed as a double Schottky barrier.[8] A positive surface charge at the immediate grain surface is assumed and this positive surface charge is compensated on both sides by a space-charge region with an extent of about 50 to 200 nm. The plausible explanation for this positive surface charge is the view that the d-orbital of titanium which are not bound to oxygen ('dangling bonds') may accept fewer electrons and thus the nuclear charge of titanium is not sufficiently balanced.[9] Caused by electrostatic interaction, this positive surface charge always leads to a build-up of negative carriers (electrons) and a depletion of positive charge carriers (electron holes) in the space-charge region.[10] In the case of *p*-type materials, the extension of this space-charge region can lead to the electrons accumulating in the space-charge region. These liberated electrons counterbalance the existing positive electron holes and therefore the hole conductivity is decreased. Comparatively, the reduction of this space-charge region causes the increment of hole conduction, leading to the reduction of the resistance.

Figure 4 shows a scanning electron microscope picture of the Mg-doped $SrTiO_3$ grain structure. It can be observed that the grain of the screen-printed Mg-doped $SrTiO_3$ thick film has a typical diameter of 200 to 500 nm. In this case, the existence of the compensating space-charge region may play an important role in determining the electrical behaviour of this material.

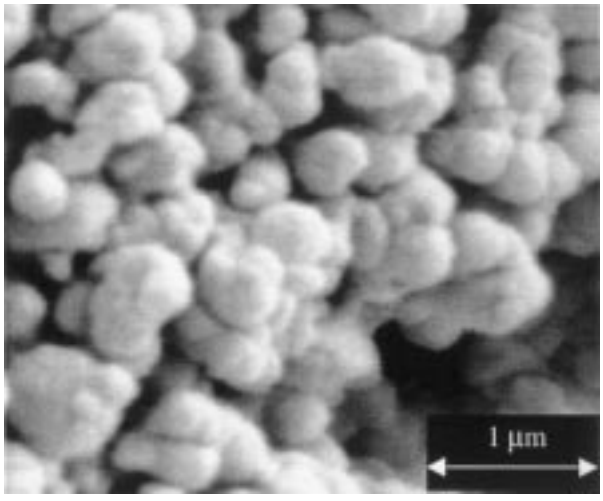

Fig. 4. SEM picture of the grain structure of a screen-printed Mg-doped $SrTiO_3$ thick film.

4 Results and Discussions

4.1 Mg-doped $SrTiO_3$ in the dry CO_2-containing atmospheres

4.1.1 Dependence of the resistance on P_{O_2} *in the dry air/*CO_2 *gas mixtures*

With aim to evaluate the influence of CO_2 on the response of the Mg-doped $SrTiO_3$ sensor, the sensor was examined by using air/CO_2 gas mixture as a dilute system and the oxygen partial pressure was changed from 10^{-4} bar (pure CO_2 gas) to 0.21 bar (air). This measurement was performed at the temperatures of 700, 720 and 750°C, respectively. The straight lines shown in Fig. 5 clearly demonstrate that the resistance of the sensor still follows a P_{O_2} dependence in an atmosphere containing N_2, O_2 and CO_2, irrespective of P_{CO_2} changes. The *m* values as defined in eqn (3) were calculated from the slope of these lines and listed in Table 1, where the R^2 value revealed the linear correlation coefficient of the curves.

It is evident that the value of *m* is very close to the theoretical value of 4, which is in good accordance with the *m* values obtained by using N_2/air

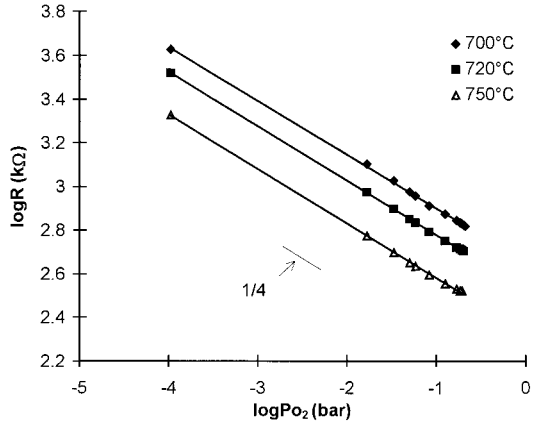

Fig. 5. Plots of log *R* versus log P_{O_2} of the sensor in the dry CO_2 air gas mixtures.

Table 1. Calculated *m* values in an atmosphere containing O_2, N_2 and CO_2

T (°C)	*700*	*720*	*750*
m	4.0633	4.0080	4.0111
R^2	0.9994	0.9999	0.9994

gas mixtures as a dilution system in our previous work.[11] This hints that the existence of CO_2 in the surrounding atmosphere will not affect the oxygen-sensing properties of the sensor and CO_2 gas can be therefore considered as the same diluting effect as N_2 gas.

4.1.2 Response of the sensor in the presence of different CO_2 partial pressures

The Mg-doped $SrTiO_3$ sensor was examined at 700°C in atmospheres of different P_{O_2} in the presence of a constant CO_2 partial pressure. First, the resistance of the sensor was measured in the atmospheres of different P_{O_2} in a sequence of (1) air (2) 1% O_2 (3) pure N_2. Then the measurement was repeated by adding a constant CO_2 content to the above three gases and the CO_2 content in gas atmospheres was set at 20, 40 and 60%, respectively. The oxygen partial pressure of the gas mixtures was determined by diluting calculation. It can be observed in Fig. 6 that the resistance of the sensor responds to the oxygen partial pressure changes regardless of different P_{CO_2} conditions and it still follows the oxygen partial pressure according to the standard expression. The experimental data ($\log R$ versus $\log P_{O_2}$) scattered at various CO_2 partial pressures roughly fit to one straight line.

4.1.3 Resistance behavior of the sensor in the dry CO_2/N_2 gas mixtures

The Mg-doped $SrTiO_3$ sensor was examined in the CO_2/N_2 gas mixtures, varying the ratio of CO_2/N_2 from 0 to 80%. The oxygen partial pressure of the CO_2/N_2 gas mixtures was measured by a commercial ZrO_2 oxygen sensor and the result was presented as the dot line in Fig. 7, which indicated that the oxygen partial pressure of the CO_2/N_2 gas mixtures was maintained almost constant since the oxygen partial pressure in pure CO_2 gas was at the same level as pure N_2. The solid line in Fig. 7 represents the resistance response of the sensor with respect to the ratios of CO_2/N_2. It is very clear that the sensor is insensitive to the different CO_2/N_2 ratios. This measurement furthermore confirms that CO_2 only plays a diluting role and has no influence on the oxygen-sensing properties of the sensor.

The above three measurements give a good proof that the Mg-doped $SrTiO_3$ sensor can still be used as oxygen sensor effectively even in an atmosphere containing CO_2 gas.

4.1.4 Creation of an uncharged surface complex in the dry CO_2-containing atmospheres

Since the Mg-doped $SrTiO_3$ sensor seems insensitive to CO_2, it is plausible to assume that the introduction of CO_2 to the gas atmosphere may not affect the oxygen-sensing bulk effect of this material and the oxygen-sensing mechanism of this material described in Section 1 still holds in an atmosphere containing CO_2. However, it is also proposed that carbondioxide molecules may be absorbed at the surface of Mg-doped $SrTiO_3$ and uncharged complexes are formed according to the following model:[12]

$$CO_{2(gas)} + O_O^{\times} \rightarrow [O_O CO_2]^{\times} \qquad (4)$$

The complex-formation process described by eqn (4) may also make it possible that a change in electronegativity at the surface occurs, which means that a fraction of an elementary charge is transferred from the absorbed CO_2 gas to the surface of Mg-doped $SrTiO_3$ and this causes some negative charge ($\delta e'$) is accumulated in the space-charge zone.[13]

$$(OCO_2)^{\bullet} \rightarrow (OCOV_O)^{\delta+} + (\delta e') + 1/2O_2 \qquad (5)$$

This negative charge will counterbalance the positive holes in this *p*-type conducting material, leading to an 'increasing' effect on the resistance of the

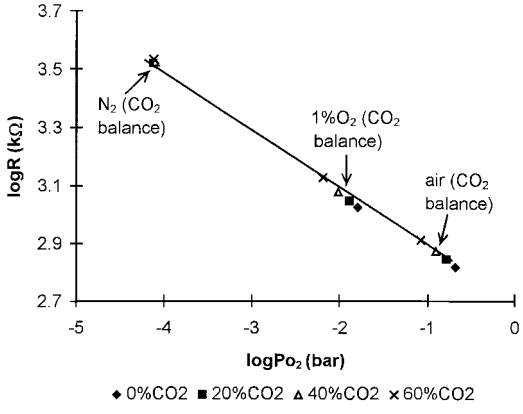

Fig. 6. $\log R$ versus $\log P_{O_2}$ of the sensor at 700°C in the presence of constant P_{CO_2} by using air/N_2/CO_2 gas mixtures.

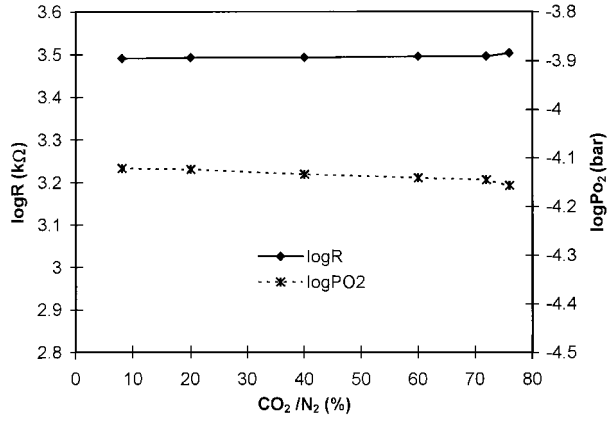

Fig. 7. Resistence behavior of the sensor at 710°C in the dry CO_2/N_2 gas mixtures.

sensor. This surface chemisorption mechanism implies that CO_2 may have a catalytic function to the oxygen-sensing properties of the sensor. This may explain why the *m* value achieved in CO_2-containing atmospheres as described in Section 4.1.1 is closer to 4 than that obtained in non-CO_2 atmospheres.

4.1.5 A comparison between the Mg-doped $SrTiO_3$ and ZrO_2 sensors in the dry CO_2/air gas mixtures

With the testing system illustrated in Section 2, it is possible to test the Mg-doped $SrTiO_3$ sensor and the ZrO_2 sensor simultaneously, keeping the experimental conditions identical. This measurement was performed in the dry CO_2/air gas mixtures and the ratio of CO_2/air in the carrier gas was changed from 0 to 92%. The oxygen partial pressure of the carrier gas was simply calculated by considering the dilution effect of CO_2 in air as shown in Fig. 8, which revealed that the logarithm of the oxygen partial pressure in this measurement was varied approximately from −0·6 to −1·8. The behaviors of these two sensors are compared in Fig. 9. The ZrO_2 sensor is observed lacking the O_2 sensing ability when the oxygen partial pressure is only slightly changed by diluting CO_2 with air and the EMF signal of the ZrO_2 sensor starts to respond to the oxygen partial pressure changes until the amount of CO_2 in the carrier gas has already exceeded 40%. By contrast, the Mg-doped $SrTiO_3$ sensor exhibits no such an insensitive region. The resistance of the Mg-doped $SrTiO_3$ sensor follows the oxygen partial pressure changes in the entire testing range. It is therefore remarkable that the Mg-doped $SrTiO_3$ sensor appears more capable to detect minute oxygen partial pressure changes.

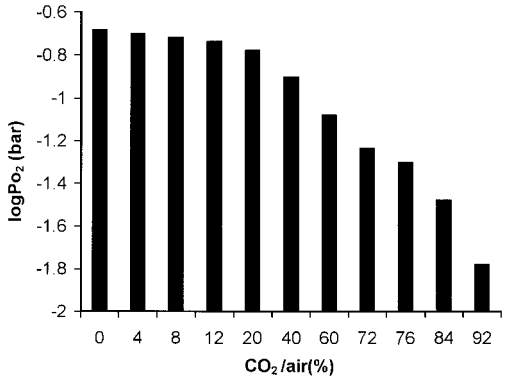

Fig. 8. Calculated oxygen partial pressure values of gases with the different CO_2/air ratios.

4.2 Mg-doped $SrTiO_3$ in the wet CO_2-containing atmospheres

4.2.1 Response to the P_{O_2} changes in the wet CO_2/air gas mixtures

The response of the sensor to the P_{O_2} changes was examined at 675°C in humidified CO_2/air gas mixtures with the CO_2 content in the carrier gas varying from 0 to 100% and the oxygen partial pressure of the testing gas was measured by a commercial ZrO_2 sensor. To make a better comparison, Fig. 10 shows the resistance of the sensor interpolated as a function of oxygen partial pressure under both dry and wet conditions. It is clear that water vapor has no influence on the response of the sensor at CO_2 concentrations below 70% since the two lines corresponding to dry and wet atmospheres, respectively, are coincident and both fit to the linearity. However, the resistance in wet conditions starts to deviate towards a lower value at a CO_2 concentration more than 70%. A severe water-vapor interference with the oxygen-sensing of the sensor is observed for the CO_2 content higher than 90% and the higher the amount of CO_2 existing in the measuring gas, the more the resistance value deviates from the straight line. This measurement was repeated at various temperatures from 675 to 775°C and this same trend occurs in the considered temperature range. The corresponding results shown in Fig. 11 confirm

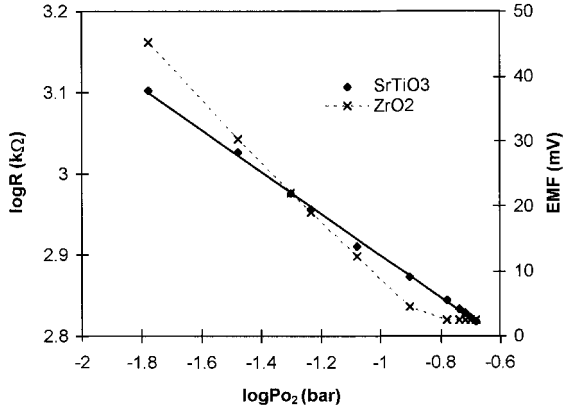

Fig. 9. Bahaviors of the Mg-doped $SrTiO_3$ sensor (700°C) and the ZrO_2 sensor in the dry CO_2/air gas mixtures.

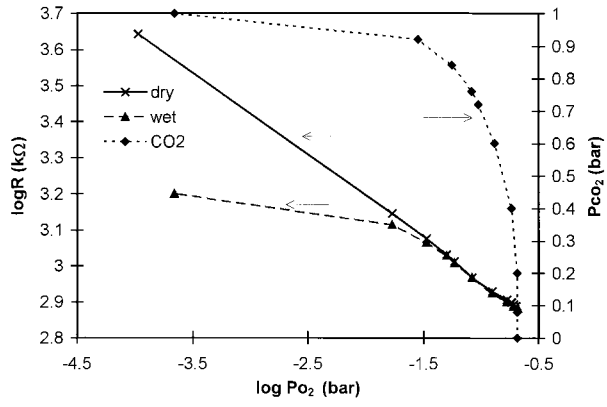

Fig. 10. Response to P_{O_2} changes of the sensor at 675°C in dry and wet atmospheres, respectively.

that the coexistence of water with a high amount of CO_2 is found to deteriorate the oxygen-sensing properties of the Mg-doped $SrTiO_3$ sensor.

4.2.2 CO_2 catalytic effect on the formation of proton conduction in wet atmospheres

It has been reported[14] that perovskite oxides may become mixed hole and proton conductors in wet atmospheres. Protons are formed by a reaction between water vapor and the oxygen vacancies present in these oxides according to:

$$H_2O(g) + V_O^{\bullet\bullet} \rightarrow O_O^{\times} + 2H_i^{\bullet} \quad (6)$$

In this case, the total conductivity is the sum of proton and hole conductivities.

$$\sigma_{total} = \sigma_P + \sigma_{H_i^{\bullet}} \quad (7)$$

The resistance of this material will therefore be decreased due to the introduction of partial proton conductivity to the total conductivity. However it is also evident that, even in wet atmospheres, hole conduction still plays a predominating role in the total conductivity and the resistance of the Mg-doped $SrTiO_3$ sensor will follow the oxygen partial pressure according to the standard expression.[15]

It is furthermore proposed[16] that CO_2 may react with water vapor to form carbonate species in an atmosphere of the coexistence of H_2O and CO_2 according to:

$$H_2O + CO_2 \Longleftrightarrow H_2CO_3 \quad (8)$$

$$H_2CO_3 \Longleftrightarrow H^+ + HCO_3^- \quad (9)$$

$$HCO_3^- \Longleftrightarrow H^+ + CO_3^{2-} \quad (10)$$

It is very obvious that reactions (6), (8)–(10) will commonly contribute to the formation of protons in an atmosphere containing both CO_2 and H_2O. If the CO_2 partial pressure is raised, reactions (8)–(10) advance toward the right, forming more protons. Consequently, the resistance of the sensor is further reduced, which may explain why the influence of CO_2 and H_2O is stronger at high CO_2 contents.

It is also plausible that this proton conducting mechanism becomes more dominant than hole conducting in wet high-CO_2 atmospheres and therefore the resistance of the sensor commences to depend on the CO_2 partial pressure according to reactions (8)–(10) instead of following the prevailing the oxygen partial pressure dependence in dry atmospheres. This assumption is verified by the fact that the P_{CO_2} dependence of the resistance of the sensor is indeed observed at high CO_2 partial pressures if replotting the data of Fig. 11 in terms of $\log R$ versus $\log P_{CO_2}$ as shown in Fig. 12.

4.2.3 A comparison between the Mg-doped $SrTiO_3$ sensor and the ZrO_2 sensor in the wet CO_2/air gas mixtures

The measurement was performed on both Mg-doped $SrTiO_3$ and ZrO_2 sensors in the wet CO_2/air gas mixtures, where the ratio of CO_2/air was changed from 0 to 92%. As the oxygen partial pressure in this gas mixture is sufficiently high ($>10^{-2}$ bar), the effect of water on the oxygen partial pressure might be neglected. The oxygen partial pressure of the carrier gas was thus calculated by only considering the dilution effect of CO_2 in air as shown in Fig. 7.

It is clear in Fig. 13 that the behavior of the ZrO_2 sensor in wet conditions is in good agreement with the results obtained in dry conditions in Fig. 9. It also exists a blind oxygen-detecting region at high oxygen partial pressure region and works properly at lower oxygen partial pressure region,

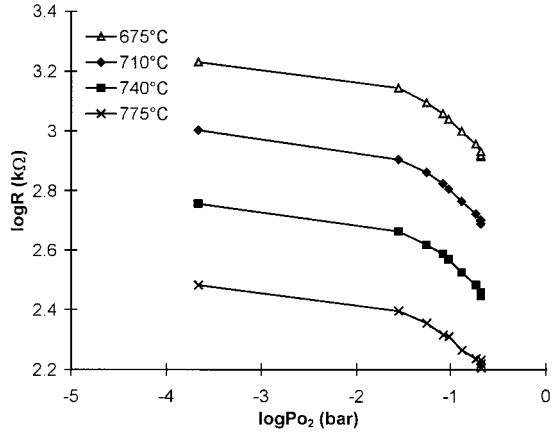

Fig. 11. Plots of $\log R$ versus $\log P_{O_2}$ of the sensor in the wet CO_2/air gas mixtures.

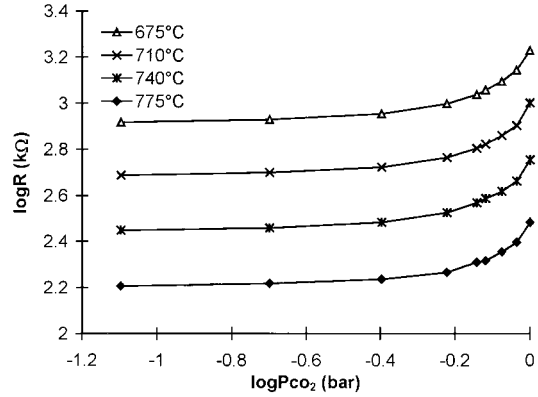

Fig. 12. Plots of $\log R$ versus $\log P_{CO_2}$ of the sensor in the wet CO_2/air gas mixtures.

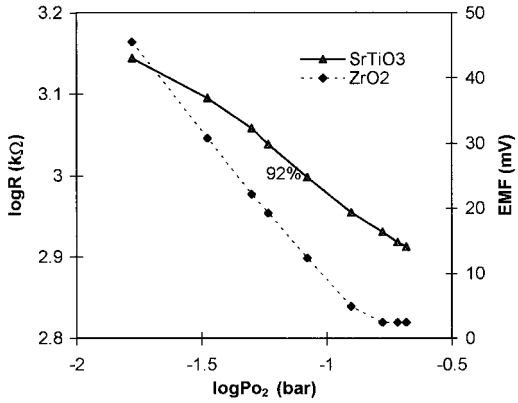

Fig. 13. Behaviors of the Mg-doped $SrTiO_3$ sensor (675 °C) and the ZrO_2 sensor in the wet CO_2/air gas mixtures.

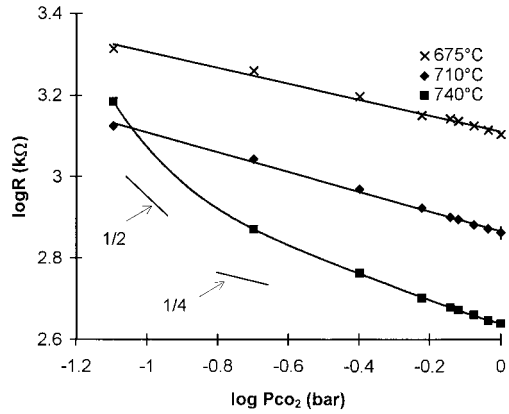

Fig. 14. Plots of log R versus log P_{CO_2} of the sensor in the wet N_2/CO_2 gas mixtures.

which demonstrates that water have little influence on the EMF signal response of the ZrO_2 sensor. However, it is found that the Mg-doped $SrTiO_3$ sensor can only operate without H_2O interference at higher oxygen partial pressure (low CO_2 concentration) region and a water interference with the oxygen-sensing is observed in lower oxygen partial pressure (high CO_2 concentration) region. By comparing the behaviors of these two sensors, it can be recognised that the ZrO_2 sensor can be considered insensitive to the presence of water vapor in the CO_2-containing atmosphere. However, the coexistence of water with high CO_2 contents may deteriorate the oxygen-sensing properties of the Mg-doped $SrTiO_3$ sensor.

4.2.4 Sensing characteristic to CO_2 in the presence of H_2O in a non-oxygen atmosphere

As mentioned above, the resistance of the Mg-doped $SrTiO_3$ sensor is found to depend on the CO_2 partial pressure at high CO_2 contents in wet atmospheres. In an attempt to make a better understanding on the CO_2-sensing characteristic of this kind of sensor in the presence of H_2O, it is necessary avoiding the cross sensitivity of the sensor to oxygen in the measurement. The measurement was thus performed in the wet N_2/CO_2 gas mixtures. The oxygen partial pressure during this measurement could be considered constant and very low as the oxygen partial pressure in pure CO_2 is at the same level as pure N_2. Figure 14 shows the relationship between the resistance of the sensor and the CO_2 partial pressures at various temperatures. It is very interesting to observe that the Mg-doped $SrTiO_3$ sensor exhibits a CO_2 partial pressure dependence in a wide CO_2 concentration range from 6 to 100%, which demonstrates that the sensor can be used to sense CO_2 sufficiently in this specific humid atmosphere.

However, the limitation for the CO_2-sensing characteristic of the sensor is that the atmosphere should be absent of oxygen. It may be ascribed to the fact that the Mg-doped $SrTiO_3$ sensor usually exhibits a primary resistance dependence on P_{O_2}, which is based on the equilibrium between the oxygen of the surrounding atmosphere and the bulk defect of this oxide according to reaction (1). Only when this equilibrium becomes insignificant in an atmosphere free from oxygen, the surface reactions between CO_2 molecules and this oxide in the presence of water vapor described by reactions[6–8] are able to play a predominating role in determining the electrical properties of this material. It is thus assumed that Mg-doped $SrTiO_3$ becomes a pure proton conductor in a non-oxygen atmosphere containing both CO_2 and H_2O.

4.2.5 CO_2-Sensing mechanism in the presence of H_2O and the absence of oxygen

A strong interaction between CO_2 and water vapor is proposed in a humid atmosphere according to:[17]

$$\mathrm{H_2O} + \mathrm{CO_2} \overset{K_1}{\longleftrightarrow} \mathrm{H_2CO_3} \overset{K_2}{\longleftrightarrow} \mathrm{H^{\bullet}} + \mathrm{HCO_3^-} \overset{K_3}{\longleftrightarrow} 2\mathrm{H^{\bullet}} + \mathrm{CO_3^{2-}} \tag{11}$$

The reaction between the water vapor and the oxygen vacancies may also be plausible:

$$\mathrm{H_2O}(g) + V_O^{\bullet\bullet} \overset{K_3}{\longleftrightarrow} + 2\mathrm{H^{\bullet}} \tag{12}$$

In this case, the charge neutrality equation can be written by:

$$2[V_O^{\bullet\bullet}] + [\mathrm{H^{\bullet}}] = [\mathrm{HCO_3^-}] + 2[\mathrm{CO_3^{2-}}] \tag{13}$$

Assuming the primary defects at lower temperatures are oxygen vacancy and bicarbonate ion, then eqn (13) is simplified as:

$$[V_O^{\bullet\bullet}] \approx [\mathrm{CO_3^{2-}}] \tag{14}$$

Equation (14) can be further expressed in a function of carbon dioxide partial pressure and water

partial pressure by including all the equilibrium constants in eqn (11) and (12):

$$[H^{\bullet}]^4 = K_1K_2K_3K_4P_{H_2O}^2P_{CO_2} \quad (15)$$

Proton conductivity is therefore given by:

$$\sigma_{H_i^{\bullet}} = e\mu_{H_i^{\bullet}}(K_1K_2K_3K_4)^{\frac{1}{4}}P_{H_2O}^{1/2}P_{CO_2}^{1/4} \quad (16)$$

Assuming the electronic hole conduction is negligible in this atmosphere and the conductivity of proton can be regarded as the total conductivity.

According to the relationship between the resistance, R, and the conductivity, σ, $R \propto 1/\sigma$, a plot of $\log R$ versus $\log P_{CO_2}$ should therefore result in a straight line with a slope$(-1/m)$ of $-1/4$ if the temperature and the water partial pressure are kept at constant:

$$\log R \propto -1/4 \log P_{CO_2} \quad (17)$$

It can be seen in eqn (14) that both the curves at 675 and 710°C appear linear with a slope $(-1/m)$ of $-1/5.1308$ and $-1/4.1356$, respectively, which is in an approximation with the theoretical value m of 4 derived above.

However, it is also evident in Fig. 14 that this linear relationship between the resistance of the sensor and the carbon dioxide partial pressure with a slope of $-1/4$ disappears when the temperature is raised to 740°C and the slope of the $\log R$ versus $\log P_{CO_2}$ curve becomes much sharper approaching to a value of $-1/2$ in low P_{CO_2} regions. It can be possibly explained based on two factors. First, high temperatures and low P_{CO_2} favor reaction (11) advancing toward to the left and it can be then modified as reaction (18). Second, reaction (12) is greatly diminished as the equilibrium constant K_4 decreases greatly with increasing temperature.[18] The formation of protons is therefore mainly due to the following reaction:

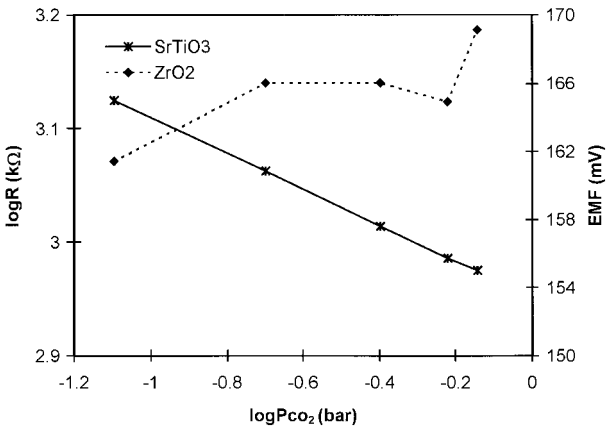

Fig. 15. Behaviors of the Mg-doped $SrTiO_3$ sensor (700°C) and the ZrO_2 sensor in the wet N_2/CO_2 gas mixtures.

$$H_2O + CO_2 \overset{K_1}{\longleftrightarrow} H_2CO_3 \overset{K_2}{\longleftrightarrow} HCO_3^- + H^{\bullet} \quad (18)$$

which gives the proton concentration by:

$$[H^{\bullet}] = K_1K_2P_{H_2O}P_{CO_2}/[HCO_3^-] \quad (19)$$

and the charge neutrality equation can be approximated as:

$$[H^{\bullet}] \approx [HCO_3^-] \quad (20)$$

Combining eqns (19) and (20) leads to

$$[H^{\bullet}] = K_1K_2P_{H_2>O}P_{CO_2} \quad (21)$$

The proton conductivity is thus given by:

$$\sigma_{H_i^{\bullet}} = e\mu_{H_i^{\bullet}}(K_1K_2)^{1/2}P_{H_2O}^{1/2}P_{CO_2}^{1/2} \quad (22)$$

which gives the theoretical value of $-1/2$ to the slope $(-1/m)$ of the plots ($\log R$ versus $\mathrm{Log}P_{CO_2}$). It is worth noting that both eqns (16) and (22) indicate the CO_2-sensing characteristic of Mg-doped $SrTiO_3$ is only associated with the presence of water vapor. This kind of sensor can be only used to detect CO_2 stably in a humid atmosphere. It is also important that the atmosphere should be free from oxygen for the sensor detecting CO_2.

4.2.6 A comparison between the Mg-doped $SrTiO_3$ sensor and the ZrO_2 sensor in the wet CO_2/N_2 gas mixtures

A comparison between the behaviors of the Mg-doped $SrTiO_3$ sensor and the ZrO_2 sensor in wet CO_2/N_2 gas mixtures was also made. As stated above, the Mg-doped $SrTiO_3$ sensor is found to exhibit an interesting CO_2-sensing characteristic in this specific situation. However no such characteristic is observed for the ZrO_2 sensor. Water and CO_2 seem no great effect on the EMF signal response of the ZrO_2 sensor and only a little changes in the EMF value is detected, which proves the ZrO_2 sensor remain its oxygen-sensing characteristic even in this specific atmosphere.

5 Conclusions

This work gives a comprehensive study on the effect of CO_2 on the response of the Mg-doped $SrTiO_3$ oxygen sensors both under dry and wet conditions. The results show that the Mg-doped $SrTiO_3$ sensor exhibits *p*-type conducting characteristic and good oxygen-sensing properties in dry atmospheres containing O_2, N_2 and even CO_2. CO_2 gas can be thus regarded as non-influential

gas in dry atmospheres and the resistance of the sensor follows the oxygen partial pressure according to the standard expression irrespective of P_{CO_2} changes. If CO_2 coexists with water vapor, the Mg-doped $SrTiO_3$ sensor can only operate properly as the oxygen sensor at CO_2 concentrations below 70% and its resistance starts to deviate from the oxygen partial pressure dependence at CO_2 concentrations more than 80%. However, the experimental results furthermore demonstrate that an interesting CO_2-sensing characteristic of the Mg-doped $SrTiO_3$ sensor is observed in a non-oxygen atmosphere containing both CO_2 and H_2O. A model based on defect chemistry, grain structures and conduction mechanisms of this material is developed to explain the experimental results satisfactorily. It is assumed that CO_2 may be absorbed at the surface of this oxide, forming an uncharged complex in the dry conditions. In the presence of H_2O, the surface reactions between CO_2 and water vapor are responsible for the formation of protons in this material, leading to the reduction of the resistance of the sensor. In a non-oxygen atmosphere containing both CO_2 and H_2O, this oxide may become a protonic conductor. A comparison between the response of the Mg-doped $SrTiO_3$ sensor and the commercial ZrO_2 sensor is also made. Generally the Mg-doped $SrTiO_3$ can be better used for oxygen-detecting in a dry CO_2-containing atmospheres. However, the ZrO_2 sensor seems more resistant to the coexistence of water vapor with CO_2 gas, which therefore shows some advantages of ZrO_2 sensor for oxygen-detecting in wet CO_2-containing atmospheres. No CO_2-sensing characteristic of the ZrO_2 sensor can be observed in this work.

References

1. Fleischer, M. and Meixner, H., Gallium oxide thin films: A new material for high temperature oxygen sensors. *Sensors and Actuators B*, 1991, **4**, 437–441.
2. Gerblinger, J., Lohwasser, W., Lampe, U. and Meixner, H., High temperature oxygen sensor based on sputtered cerium oxide. *Sensors and Actuators B*, 1995, **26–27**, 93–96.
3. Zhou, X, Toft Sørensen, O. and Xu, Y., Defect structure and oxygen sensing properties of Mg-doped $SrTiO_3$ thick film sensors. *Sensors and Actuators B*, 1997, **41**, 177–182.
4. Moseley, P. T., Materials selection for semiconductor gas sensors. *Sensors and Actuators B*, 1992, **6**, 149–156.
5. Gerblinger, J., Lampe, U. and Meixner, X., Cross-sensitivity of various doped strontium titanate films to CO, CO_2, H_2, H_2O and CH_4. *Sensors and Actuators B*, 1994, **18–19**, 529–534.
6. Zheng, Hong, Jensen, H., Toft Sørensen, O., Preparation of fine $SrTiO_3$ and $Sr(Mg_{0.4}Ti_{0.6})O_{3-\delta}$ perovskite ceramic powders by a sol–precipitation process. RISØ-I-1296 (EN), Risø National Laboratory, Denmark, 1998.
7. Meixner, H., Gerblinger, J. and Fleischer, M., Sensors for monitoring environmental pollution. *Sensors and Actuators B*, 1993, **15–16**, 45–54.
8. Chiang, Y. M. and Tagaki, T., Grain-boundary chemistry of barium strontium titanate: I, high-temperature equilibrium space charge. *J. Am. Ceram. Soc.*, 1990, **73**, 3278–3285.
9. Tragut, C., The kinetics of fast oxygen sensors. *VDI-Verlag*. 1992, **8**(291).
10. Gerblinger, J., Hausner, M. and Meixner, H., Electric and kinetic properties of screen-printed strontium titanate films at high temperatures. *J. Am. Soc.*, 1995, **78**(6), 1451–1456.
11. Zheng, Hong, Jensen, H., Toft Sørensen, O., DMS Vintermdet, Rudkøbing, Denmark, 1998.
12. Meixner, H., Gerblinger, J., Lampe, U. and Fleischer, M., Thin-film gas sensors based on semiconducting metal oxides. *Sensors and Actuators B*, 1995, **23**, 119–125.
13. Baltes, H., Göpel, W., Hesse, J., *Sensors Update*, vol. 2. VCH Verlasgesellschaft mbH, Weinheim, 1997.
14. Sutija, D. P., Norby, T. and Björnbom, P., Transport number determination by the concentration-cell/open-circuit voltage method for oxides with mixed electronic, ionic and protonic conductivity. *Solid State Ionics*, 1995, **77**, 167–174.
15. Zheng, Hong, Jensen, H., Sørensen, O. T., Influence of water vapor on the response of Mg-doped $SrTiO_3$ ceramic oxygen sensors. *J. Electroceramics*.
16. Jinghong, Han, Dafu, Cui, Yating, Li, Jine, Cai, Zheng, Dong and Hong, Zhang, A new type of transcutaneous Pco_2 sensor. *Sensors and Actuators B*, 1995, **24–25**, 156–158.
17. Varlan, A. R. and Sansen, W., Micromachined conductometric $p(CO_2)$ sensor. *Sensors and Actuators B*, 1997, **44**, 309–315.
18. Uchida, H., Yoshikawa, H., Esaka, T., Ohtsu, S. and Iwahara, H., Formation of protons in $SrCeO_3$-based proton conducting oxides. Part II. Evaluation of proton concentration and mobility in Yb-doped $SrCeO_3$. *Solid State Ionics*, 1989, **36**, 89–95.